Kinetic Study of the Ring-Opening Metathesis Polymerization of Ionically Functionalized Cyclooctatetraenes

Brandi L. Langsdorf, Xin Zhou, and Mark C. Lonergan*

Department of Chemistry and the Materials Science Institute, University of Oregon, Eugene, Oregon 97403

Received December 5, 2000; Revised Manuscript Received February 12, 2001

ABSTRACT: The ring-opening metathesis polymerizations of alkylammonium and sulfonate functionalized cyclooctatetraenes (RCOT, R = $CH_2CH_2SO_3TMA$ or $CH_2CH_2NMe_3OTf$, OTf = $CF_3SO_3^-$, TMA = Me_4N^+) with the well-defined tungsten catalyst W=CH(*o*-C_6H_4OMe)(NC_6H_5)[$OCCH_3(CF_3)_2]_2$(THF) (THF = tetrahydrofuran) were investigated. The polymerizations exhibited first-order decay in monomer concentration and slow initiation relative to propagation, and for $COTCH_2CH_2SO_3TMA$ where studies were possible, molecular weights largely independent of the extent of the reaction and initial reaction conditions. The central kinetic feature was the observation of a pseudo-first-order rate constant inversely proportional to the *initial* monomer concentration, suggesting some form of inhibition. Furthermore, the polymerization of $COTCH_2CH_2NMe_3OTf$ is inhibited by the addition of TBAOTf (TBA = Bu_4N^+). The apparent inhibition is discussed in terms of the potential for ion pairing or anion coordination to the catalyst center.

Introduction

Tungsten and molybdenum imido alkylidene complexes are powerful catalysts that have been reported to initiate controlled ring-opening metathesis polymerizations that offer precise command over polymer structure.[1−6] However, their affinity for Lewis bases and Wittig-like reactivity has led to concerns over their functional group tolerance. Recently, several groups have reported the tolerance of well-defined tungsten and molybdenum catalysts toward a variety of functional groups containing heteroatoms such as oxygen, nitrogen, halogens, and silicon.[1,2,7,8] Despite earlier reports of catalyst poisoning by these substituents in classical catalytic systems, functionalized norbornenes and norbornadienes have undergone ring-opening metathesis polymerization to give polymer yields as high as 98% with polydispersities near the living threshold at 1.04.[9]

The use of well-defined tungsten and molybdenum imido alkylidene catalysts in the synthesis of polyelectrolytes has received little attention. In the few examples reported, the catalyst was reacted with a nonionic monomer, and the resulting polymer subsequently reacted to form the desired polyelectrolyte. For instance, Schitter et al. recently reported the use of protecting group chemistry in the synthesis of carboxylic acid functionalized polyelectrolytes with molybdenum alkylidene catalysts.[10] Zhang et al. have prepared a cationic conjugated ionomer using cyclopolymerization of *N*-hexyldipropargylamine initiated with a molybdenum alkylidene followed by post-polymerization quaternization.[11] Wagaman and Grubbs have prepared a dicarboxylate poly(1,4-phenylenevinylene) through a precursor route relying on the ring-opening metathesis polymerization (ROMP) of substituted nonionizable barrelenes with a molybdenum imido alkylidene catalyst.[12]

Recently, we reported the direct synthesis of polyacetylene ionomers from ionically functionalized cyclooctatetraenes using W=CH(*o*-C_6H_4OMe)(NC_6H_5)-[$OCCH_3(CF_3)_2]_2$(THF) (**1**, THF = tetrahydrofuran). Our interest in these materials stems from the unique possibilities these highly conjugated, soluble polyelectrolytes may afford in the fabrication of new types of conjugated polymer interfaces.[13,14] Key to these applications is the ability to control polymer structure. Here, we report a more detailed study of the kinetics for the polymerization of ionically functionalized cyclooctatetraenes undertaken to assess the level of control that might be possible over polymer microstructure. These studies were also pursued to investigate the distinct kinetic features that can arise in the metathesis polymerization of ionizable monomers by a well-defined alkylidene catalyst.

The direct polymerization of ionizable monomers by well-defined tungsten and molybdenum imido alkylidene catalysts raises a number of questions. These catalysts have been shown to coordinate a large range of Lewis bases, thus raising concerns over anion coordination in the direct polymerization of ionically functionalized monomers. Whereas the coordination of select ligands can be used to exert enhanced control over polymerizations by influencing the relative rate of initiation vs propagation,[5,6,15] in certain cases the coordination of Lewis bases can completely inactivate the catalyst.[2] Ion−ion interactions may also have a pronounced effect. The interactions between charged species is known to influence a wide range of chemical reactions.[16] Polymerizations involving ionic species may be influenced, for instance, by ion pairing/clustering equilibria as observed in ionic polymerizations,[17] by interactions of ionic monomers with the growing chains in a manner analogous to the penultimate effect in ionic polymerizations,[18] or by the organizing influence of the growing polymer chains as in so-called "polyelectrolyte catalysis".[19]

Results

General Observations. Monofunctionalized cyclooctatetraene [RCOT, R = $CH_2CH_2SO_3TMA$ (**M$_A$**) or CH_2-CH_2NMe_3OTf (**M$_C$**), OTf = $CF_3SO_3^-$, TMA = Me_4N^+] was treated with **1**[4,20] in chloroform ($CHCl_3$), as shown

10.1021/ma0020685 CCC: $20.00
Published on Web 03/17/2001

Scheme 1. Ring-Opening Metathesis Polymerization of Ionically Functionalized Cyclooctatetraenes

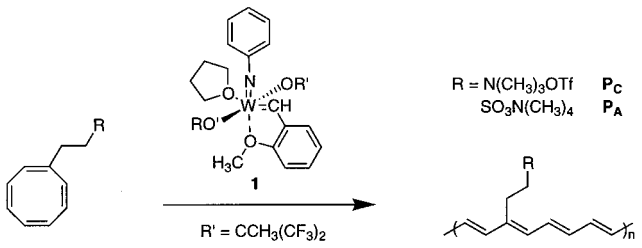

in Scheme 1, to produce a poly(RCOT) bearing an ionic functionality by ring-opening metathesis polymerization. Upon initiation, the color of the polymerization medium changed from the light yellow of the monomer to the dark blue of the precipitating polymer. As previously reported, both $\mathbf{P_C}$ and $\mathbf{P_A}$ are dark blue solids with the thermodynamically stable predominately trans form soluble in a variety of highly polarizable solvents. For example, $\mathbf{P_C}$ and $\mathbf{P_A}$ dissolve in dimethyl sulfoxide (DMSO) and *N*,*N*-dimethylformamide (DMF).[13] Additionally, $\mathbf{P_A}$ is also soluble in methanol and ion exchange to the sodium salt imparts water solubility.

Initiation. The ^{1}H and ^{13}C NMR spectra of uninitiated **1** in $CDCl_3$ display characteristic resonances corresponding to the benzylic alkylidene proton at 10.5 ppm (H_α) and 234.5 ppm (C_α), respectively. Upon monomer insertion, the original uncoupled benzylic alkylidene proton resonance represented by a singlet is expected to be replaced by the vinylic alkylidene proton resonance of the growing polymer chain. The vinylic alkylidene proton would be observed as a doublet in the ^{1}H NMR spectrum. A vinylic alkylidene resonance corresponding to the propagating species was not observed in the polymerization of $\mathbf{M_A}$ and $\mathbf{M_C}$ or during the polymerization of a variety of nonionic RCOTs [R = $Si(CH_3)_3$ (TMS), $CH_2CH(CH_3)_2$, $CH_2CH_2SO_3CH_3$]. The position, intensity, and splitting pattern of the original uninitiated alkylidene resonance remained largely unchanged in the proton spectrum. For example, during the 10 h polymerization of $\mathbf{M_A}$ ($[\mathbf{M_A}]_0$ = 124 mM, $[C]_0[\mathbf{1}]_0$ = 25 mM) through 90% monomer conversion, the intensity of the ^{1}H alkylidene (H_α) singlet resonance was constant. In separate experiments, during the polymerization of each $\mathbf{M_A}$ and $\mathbf{M_C}$ in $CDCl_3$, a small resonance, corresponding to less than 1% of the original alkylidene intensity, did appear roughly 0.1 ppm downfield from the original peak within 1 h of the start of the polymerization reaction. A similar resonance was observed in control experiments conducted to observe the stability of **1** in the reaction solvent at 25 °C; thus, this signal is attributed to an unidentified decomposition product of the catalyst. Lack of perceivable change of the alkylidene region during consumption of monomer indicates that the rate of initiation of **1** is much slower than the rate of propagation or that a minor unobservable impurity in the catalyst is the active species.

Experiments designed to detect the possible presence of a highly active impurity were performed based on the idea that any small amount of a rapidly initiating impurity would be depleted quickly. To test for such an impurity, individual polymerizations of either $\mathbf{M_C}$ or $\mathbf{M_A}$ were conducted, allowing the monomer to be completely consumed as confirmed by ^{1}H NMR spectroscopy. After complete conversion of the monomer, the polymer was isolated from the reaction solution, and an additional aliquot of the original monomer was added to the polymer-free supernatant. In both experiments, the second aliquot of monomer was also consumed. Consumption of the second aliquot of monomer refutes the presence of a rapidly initiating impurity and instead suggests that initiation occurs much more slowly than propagation for the ROMP of $\mathbf{M_C}$ and $\mathbf{M_A}$.

Overall Reaction Kinetics. Figure 1 shows a comparison of first-order (ln $[M]/[M]_0$ vs time) and zero-order ($[M]/[M]_0$ vs time) plots for the polymerization of a nonionic monomer TMSCOT ($[M]_0$ = 125 mM, $[C]_0$ = 10 mM) and the ionic monomers, $\mathbf{M_C}$ ($[M]_0$ = 140 mM, $[C]_0$ = 17 mM) and $\mathbf{M_A}$ ($[M]_0$ = 125 mM, $[C]_0$ = 25 mM), at ambient temperature. ^{1}H NMR spectroscopy was used to follow the course of the polymerization by monitoring the resonances corresponding to the protons of the cyclooctatetraene ring, appearing as a broad multiplet from 5.6 to 5.9 ppm. In the case of the ionically functionalized cyclooctatetraenes, precipitation of the polymer minimizes contributions from the growing polymer chain allowing clean integration of all of the monomer ring protons. For TMSCOT, however, the soluble polymer product appears in the same region, 5.8−7.2 ppm, as the ring protons of the unreacted monomer, thereby complicating integration. Quantization for TMSCOT was accomplished by using only an upfield portion of the monomer ring multiplet, corresponding to four protons that remained relatively unobscured until late in the polymerization.

The nonionic monomer exhibits zero-order decay of monomer concentration as has been reported for the polymerization of norbornene with **1**.[4,8,21] In contrast, $\mathbf{M_C}$ and $\mathbf{M_A}$ exhibit apparent first-order decays of monomer concentration. The variation in apparent reaction order implies a substantial difference in the reaction mechanisms between ionic and nonionic monomers.[22] The relative polymerization rates at early reaction times when the monomer concentration is roughly constant are 9.4×10^{-5}, 1.5×10^{-6}, and 3.8×10^{-6} M s^{-1} for $\mathbf{M_C}$, $\mathbf{M_A}$, and TMSCOT, respectively. Even allowing for the variance in reaction conditions, the cationic monomer is consumed much more quickly than its nonionic counterpart and still more quickly than $\mathbf{M_A}$. The polymerization of $\mathbf{M_A}$ was observed to be slower than TMSCOT, even in the presence of twice as much catalyst.

To further explore the reaction order, a series of polymerizations of $\mathbf{M_A}$ and $\mathbf{M_C}$ initiated by **1** were conducted with various initial monomer and catalyst concentrations. These experiments were conducted gravimetrically rather than spectroscopically due to initial concerns regarding the ability to obtain clean integration of potentially overlapping resonances and the desire to isolate polymer at various stages in the reaction for further characterization. In these gravimetric studies, the rate of monomer consumption was measured by determining the amount of polymer produced as a function of time. The fraction of polymer soluble in the reaction medium was very small for each aliquot.

The polymer mass obtained provides an accurate measure of monomer consumption only in the absence of side reactions that consume monomer and an upper limit otherwise. The most probable side reaction would be the intramolecular reaction of the propagating catalyst with the growing polymer chain to extrude arenes. This nonproductive, backbiting reaction results in the

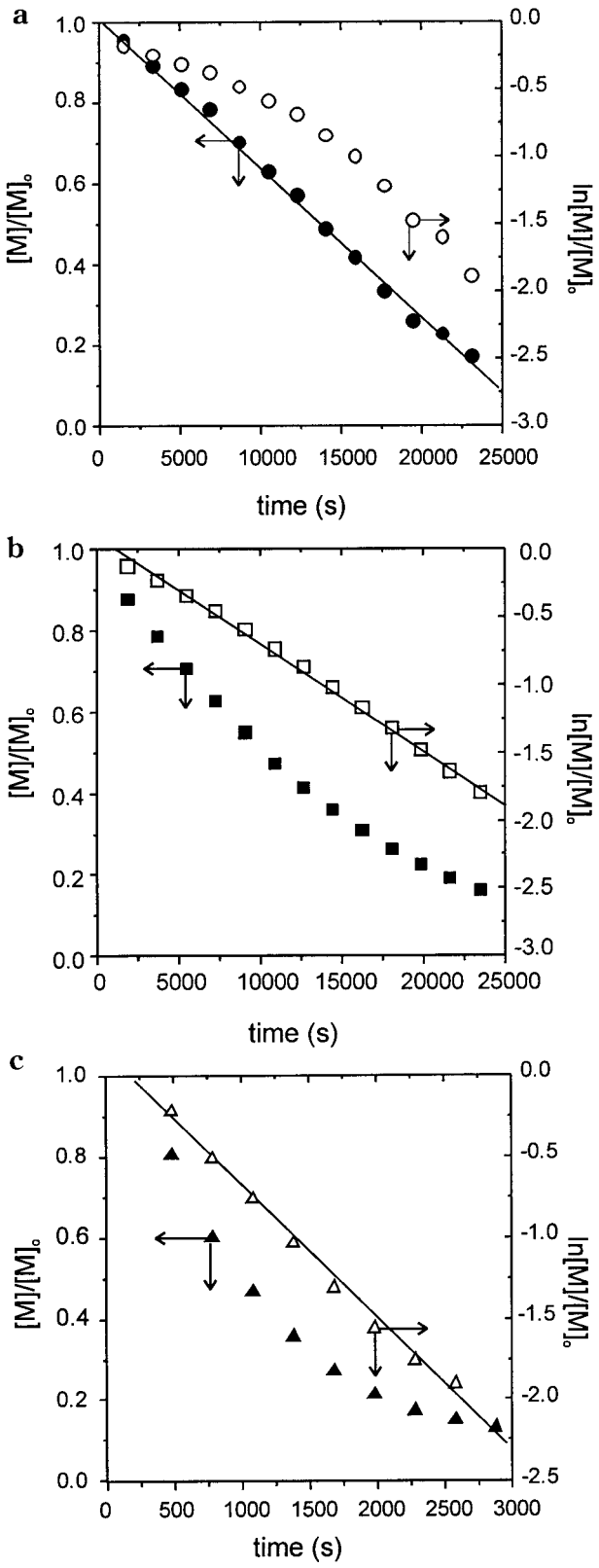

Figure 1. Polymerization in $CHCl_3$ at 23 °C as a function of time monitored by ^{1}H NMR spectroscopy: (a) TMSCOT; a first-order representation (○) and zero-order representation (●). (b) $\mathbf{M_A}$; a first-order representation (□) and zero-order representation (■). (c) $\mathbf{M_C}$; a first-order representation (△) and zero-order representation (▲).

reduction of the chain length by the reaction of the propagating catalyst to split out small molecules via intramolecular olefin metathesis. Lewis bases coordinated to the catalyst center in combination with a

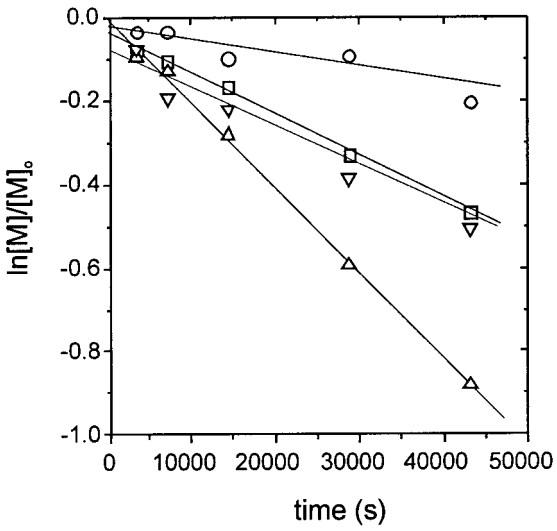

Figure 2. First-order representation of $\ln[M]/[M]_0$ as a function of time for the polymerization of $\mathbf{M_A}$ in $CHCl_3$ at 23 °C for $[M]_0$ and $[C]_0$ listed in Table 1; $\mathbf{1P_A}$ (○), $\mathbf{2P_A}$ (□), $\mathbf{3P_A}$ (▽), and $\mathbf{4P_A}$ (△). Although the data for $\mathbf{M_A}$ shown in this graphic do not span a sufficient range of concentration to clearly distinguish a first-order from zero-order decay in monomer, the ^{1}H NMR spectroscopic studies shown in Figure 1 clearly show a first-order decay.

Table 1. Reaction Conditions and Observed Rate Constants for the Reaction of 1 with $\mathbf{M_A}$, $\mathbf{M_C}$, and $\mathbf{M_C}$ in the Presence of TBAOTf at 23 °C in $CHCl_3$ To Produce Polymers $\mathbf{P_A}$, $\mathbf{P_C}$, and $\mathbf{P_{C+L}}$, Respectively

	$[M]_0$ (mmol/L)	$[C]_0$ (mmol/L)	$[TBAOTf]_0$ (mmol/L)	$[M]_0/[C]_0$	k_{obs} (s^{-1})
$\mathbf{1P_A}$	370	8.1		46	4.0×10^{-6}
$\mathbf{2P_A}$	180	10		18	1.0×10^{-5}
$\mathbf{3P_A}$	380	16		24	1.0×10^{-5}
$\mathbf{4P_A}$	180	17		11	2.0×10^{-5}
$\mathbf{1P_C}$	480	3.5		140	4.5×10^{-5}
$\mathbf{2P_C}$	460	7.2		64	1.7×10^{-4}
$\mathbf{3P_C}$	250	3.9		63	1.9×10^{-4}
$\mathbf{4P_C}$	270	6.5		42	3.3×10^{-4}
$\mathbf{5P_C}$	270	8.9		30	5.1×10^{-4}
$\mathbf{1P_{C+L}}$	230	8.5	380	28	6.2×10^{-5}
$\mathbf{2P_{C+L}}$	280	4.5	150	63	4.3×10^{-5}
$\mathbf{3P_{C+L}}$	250	4.0	64	63	6.2×10^{-5}

coordinatively saturated metal center, such as in **1**, are postulated to limit the amount of backbiting and in some cases prevent it altogether.[4,6] During the polymerization of $\mathbf{M_C}$ and $\mathbf{M_A}$, only limited backbiting products were observed by ^{1}H NMR spectroscopy. Backbiting products appeared at the beginning of the reaction and gradually increased in concentration throughout the course of the polymerization. For example, after 15 min of the reaction of **1** with $\mathbf{M_C}$ in $CHCl_3$ at 25 °C, resonances appeared between 7.2 and 7.5 ppm ascribed to the arene products of intramolecular olefin metathesis. The rate of appearance of these resonances tapered off as the reaction proceeded, coming to a halt as the monomer was completely depleted. The intramolecular metathesis is therefore associated only with actively propagating polymer. The total amount of backbiting product amounted to less than 5% of the initial monomer concentration.

Table 1 shows the initial monomer and catalyst concentrations investigated for polymerizations of $\mathbf{M_A}$ and $\mathbf{M_C}$ in $CHCl_3$. Figures 2 and 3 present the results of these polymerizations in the form of first-order plots of the monomer concentration with respect to the

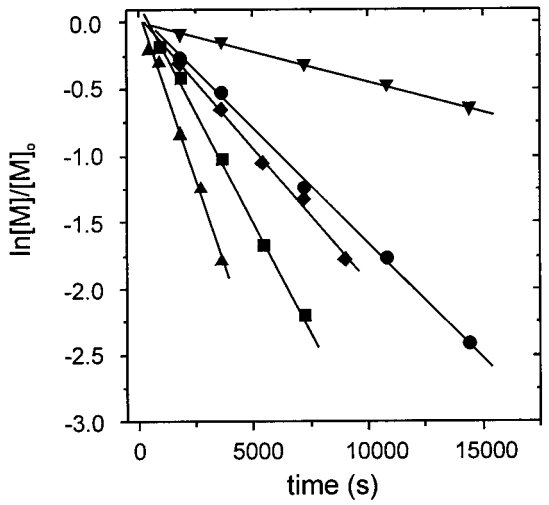

Figure 3. First-order representation of $\ln[M]/[M]_0$ as a function of time for the polymerization of $\mathbf{M_C}$ in $CHCl_3$ at 23 °C for $[M]_0$ and $[C]_0$ listed in Table 1: $\mathbf{1P_C}$ (▼), $\mathbf{2P_C}$ (●), $\mathbf{3P_C}$ (◆), $\mathbf{4P_C}$ (■), and $\mathbf{5P_C}$ (▲).

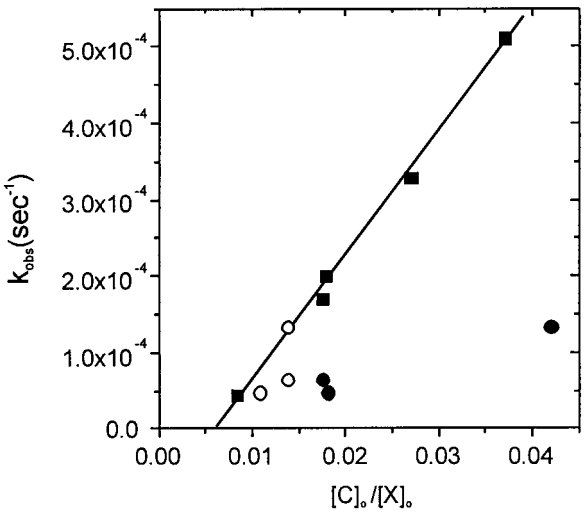

Figure 4. Plot of k_{obs} vs $[C]_0/[X]_0$ for the polymerization of $\mathbf{M_C}$ initiated by **1** with (circle) or without (square) additional TBAOTf in $CHCl_3$ at 23 °C where $[X]_0 = [\mathbf{M_C}]_0$ (solid symbols) and $[X]_0 = [S]_0 = [\mathbf{M_C}]_0 + [TBAOTf]_0$ (open symbols).

polymerization reaction time. As observed with the ^1H NMR spectroscopy experiments, the polymerizations of the ionic monomers are seen to follow first-order decays in monomer concentration for all of the initial catalyst and monomer concentrations investigated throughout the extent of the reactions.

Despite the significant differences in the rates of monomer consumption during the polymerizations of $\mathbf{M_A}$ and $\mathbf{M_C}$, much about their reaction behavior is similar. For both $\mathbf{M_A}$ and $\mathbf{M_C}$, comparison of the trials with the same monomer concentration $\mathbf{1P_A}$ and $\mathbf{3P_A}$ in Figure 2 or $\mathbf{1P_C}$ and $\mathbf{2P_C}$ in Figure 3, for example, demonstrates that increasing the catalyst concentration increases the slope of these first-order plots, thus providing a pseudo-first-order rate constant, k_{obs}, for the consumption of monomer that increases with increasing catalyst concentration. The observation of a linear first-order plot in monomer, by definition, requires k_{obs} to be independent of the change in monomer concentration for a given set of polymerization conditions. Surprisingly, however, comparison of trials with the same initial catalyst concentration but different initial monomer concentrations, for example $\mathbf{1P_A}$ and $\mathbf{2P_A}$ or $\mathbf{1P_C}$ and $\mathbf{3P_C}$, shows that k_{obs} depends on *initial* monomer concentration, with k_{obs} decreasing as the initial monomer concentration increases! As such, similar k_{obs} can be observed for polymerizations carried out at different catalyst concentrations, for example, $\mathbf{2P_A}$ and $\mathbf{3P_A}$ or $\mathbf{2P_C}$ and $\mathbf{3P_C}$. Comparison of the reaction conditions for $\mathbf{2P_A}$ and $\mathbf{3P_A}$ or $\mathbf{2P_C}$ and $\mathbf{3P_C}$ suggests that k_{obs} depends on the ratio of the initial catalyst concentration to the initial monomer concentration. Indeed, k_{obs} is observed to be linearly related to $[C]_0/[M]_0$ (Figure 4, solid squares), thereby suggesting an empirical rate law of the following form:

$$\frac{-\mathrm{d}[M]}{\mathrm{d}t} = k\frac{[C]_0}{[M]_0}[M] \qquad (1)$$

that yields $k_{obs} = k[C]_0/[M]_0$, where k is a constant. In eq 1, $[M]_0$ represents initial monomer concentration, and [M] represents the time-dependent monomer concentration; therefore, the two are only equivalent at the start of the reaction. The empirical rate law (eq 1) predicts first-order decay in monomer concentration for a given reaction and zero-order dependence of the initial reaction rate on monomer concentration for a series of reactions at constant catalyst concentration.

Influence of Ionic Additives. The observation of the empirical rate law (eq 1) suggests that the rate of polymerization is inhibited by the monomer. As discussed in greater detail below, the unusual empirical rate law could result from ion-pairing effects, since the ionic strength of the solution depends on the initial monomer concentration, or perhaps is due to direct coordination of the anion to the active catalyst center. To investigate the influence of anion coordination or ion pairing, the kinetics of the reaction of **1** with $\mathbf{M_C}$ in the presence of tetrabutylammonium triflate (TBAOTf) were investigated. Direct interactions between TBAOTf and **1** in $CDCl_3$ were difficult to observe. The addition of a large excess of TBAOTf to **1** (1.0 mmol of TBAOTf and 0.042 mmol of **1** relative to an internal standard) did not result in a perceivable change in the ^1H NMR spectrum of **1** in $CDCl_3$ and produced only a minor change in ^{13}C NMR spectrum [$\Delta(C_\alpha) = 0.5$ ppm, collected using a 500 MHz NMR]. The same experiment was also conducted with the THF-free analogue of **1**, which because of its increased electron deficiency and lower coordination is expected to be more highly reactive with Lewis bases. Again, upon addition of TBAOTf no significant shift was observed for either the H_α or C_α resonance.

Polymerization studies of $\mathbf{M_C}$ in the presence of TBAOTf were performed as described for the studies above with the exception that both $\mathbf{M_C}$ and TBAOTf were dissolved in $CHCl_3$ prior to the addition of the catalyst to the reaction mixture. The concentrations of monomer and catalyst were chosen to model previous polymerizations of $\mathbf{M_C}$ without added TBAOTf. The relevant reaction conditions are listed in Table 1.

Figure 5 compares first-order plots for the polymerization of $\mathbf{M_C}$ with and without added TBAOTf for otherwise similar reaction conditions. Polymerization of $\mathbf{M_C}$ in the presence of TBAOTf exhibits first-order decay in monomer concentration and substantially slowed reactivity.[23] These results suggest a competitive inhibition by the coordinating OTf anion or some less specific ion-pairing effect. The studies with and without added

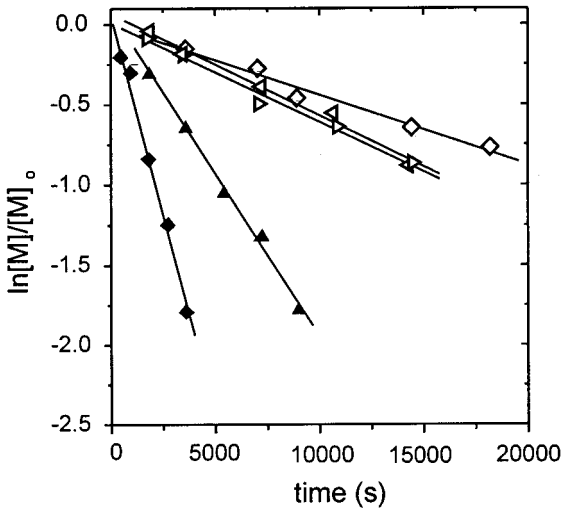

Figure 5. First-order representation of $\ln[M]/[M]_0$ as a function of time for the polymerization of $\mathbf{M_C}$ in the presence of TBAOTf in $CHCl_3$ at 23 °C compared to the polymerization of $\mathbf{M_C}$ in the absence of added TBAOTf under similar conditions (see Table 1 for specifics): $\mathbf{3P_C}$ (◆), $\mathbf{5P_C}$ (▲) $\mathbf{1P_{C+L}}$(◇), $\mathbf{2P_{C+L}}$ (left triangle open), $\mathbf{3P_{C+L}}$ (right triangle open).

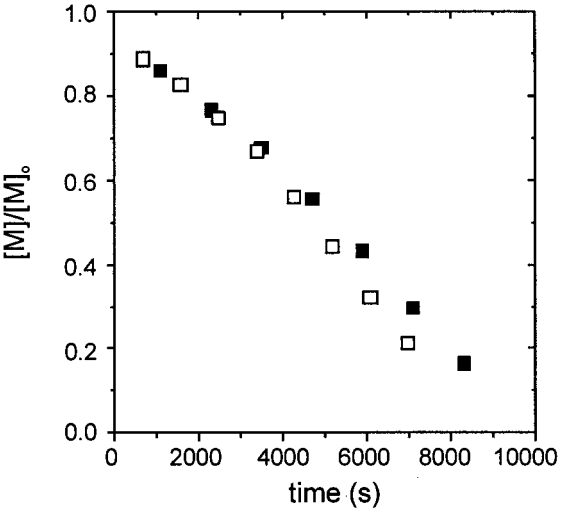

Figure 6. $[M]/[M]_0$ for the polymerization of TMSCOT in $CHCl_3$ at 23 °C as a function of time with TBAOTf (□; $[M]_0$ = 385 mM, $[C]_0$ = 37 mM, [TBAOTf] = 277 mM) and without added TBAOTf (■; $[M]_0$ = 330 mM, $[C]_0$ = 43 mM).

TBAOTf can be consistently incorporated into a single empirical rate law:

$$\frac{-\mathrm{d}[M]}{\mathrm{d}t} = k\frac{[C]_0}{[S]_0}[M] \qquad (2)$$

where $[S]_0$ is the total initial concentration of salt. Figure 4 shows the pseudo-first-order rate constants for the polymerizations of $\mathbf{M_C}$ with and without added TBAOTf vs $[C]_0/[S]_0$, where $[S]_0 = [\mathbf{M_C}]_0 + [\mathrm{TBAOTf}]_0$ in this case. As can be seen, the use of the total salt concentration qualitatively linearizes all of the studies on $\mathbf{M_C}$.

The addition of TBAOTf did not significantly influence the polymerization of the neutral monomer TMSCOT in chloroform ($[M]_0$ = 385 mM, $[C]_0$ = 37 mM, $[\mathrm{TBAOTf}]_0$ = 277 mM). Figure 6 shows the kinetics for the polymerization of TMSCOT, followed by ^{1}H NMR spectroscopy, with and without the addition of TBAOTf. The polymerization kinetics remain zero-order in monomer, and the rate of polymerization is essentially unchanged.

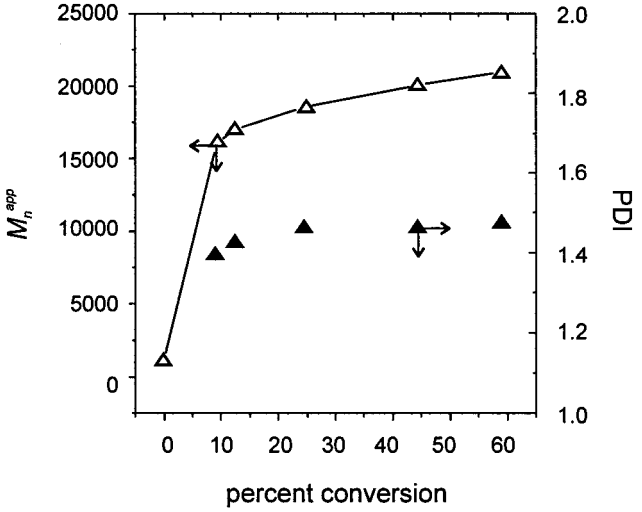

Figure 7. $\bar{M}_n^{app}$ (Δ) and PDI of $\mathbf{4P_A}$ (▲) in 0.4% TBAOTf/DMSO vs TMAPSS standards. The initial time point (t = 0) is an upper limit of the M_n^{app} of the monomer.

Evolution of Molecular Weight and Optical Absorption. Attempts were made to characterize the molecular weights of both $\mathbf{P_A}$ and $\mathbf{P_C}$ by gel permeation chromatography. With either pure DMF or DMSO as eluent, $\mathbf{P_A}$ is excluded from the chromatography columns, while $\mathbf{P_C}$ is retained on the columns, presumably due to strong interactions with residual carboxylate groups of the stationary phase. Addition of TBAOTf or $TMABF_4$ to adjust the ionic strength of the eluent permitted separation of $\mathbf{P_A}$ by the columns; however, chromatographic conditions for the separation and characterization for $\mathbf{P_C}$ could not be identified.[24] $TMABF_4$ was used for the characterization of $\mathbf{P_A}$ to eliminate the possibility of ion exchange between the polymer and the eluent. The optimum ionic strength of the eluent for the characterization of $\mathbf{P_A}$ was determined by conducting chromatography under increasing ionic strengths. An increase in retention time of $\mathbf{P_A}$ on the chromatography column was observed as the salt concentration of the eluent was increased, with a plateau reached at 0.4% w/v $TMABF_4$ in DMF, the concentration used to obtain the results reported herein. Apparent molecular weights are reported relative to poly(styrenesulfonate) standards and should be interpreted with the standard cautions regarding the use of size exclusion chromatography relative to a dissimilar polymer. We view the results primarily from the viewpoint of trends in molecular weight and polydispersities, rather than as absolute measures of molecular weight. The number-averaged, apparent molecular weight $\bar{M}_n^{app}$ as a function of the percent conversion of monomer for a representative polymerization, $\mathbf{4P_A}$, is shown in Figure 7. The molecular weight increases sharply from the monomer molecular weight and then plateaus at an apparent molecular weight $\bar{M}_n^{app} \approx 20\,000$ ($\bar{X}_n^{app} \approx 70$). The polydispersity of the polymer remains constant throughout the polymerization at approximately 1.5. The ultimate molecular weight for the entire $\mathbf{P_A}$ series was found to be independent of the initial monomer and catalyst concentrations with $\bar{M}_n^{app} \approx 20\,000 \pm 2000$.

Absorbance spectroscopy was conducted upon completion of each polymerization series. A single absorbance

maximum was observed for each time point and is attributed to the thermodynamically favored trans conformation of the polymer. The polymerization is sufficiently long to allow isomerization from the original cis conformation.[5,13] The polymers produced in the kinetic experiments described above for the $\mathbf{P_A}$ series demonstrate rapid evolution of λ_{max} values (DMSO) similar to the behavior of $\bar{M}_n^{app}(t)$. After only 9% monomer conversion, $\mathbf{4P_A}$ displays a λ_{max} value of 570 nm, with the λ_{max} values in DMSO remaining relatively constant over the course of the polymerization, reaching a λ_{max} value of 590 nm when polymerization of the final aliquot is terminated at 58% monomer conversion. Absorbance maxima for $\mathbf{P_C}$ also reach a plateau within the initial aliquot period displaying single λ_{max} values of 605−615 nm in DMSO depending on the reaction conditions.[25]

Discussion

Many ring-opening metathesis polymerizations using tungsten and molybdenum imido alkylidene complexes proceed in a controlled or "living" fashion where fast initiation and the absence of termination lead to linear growth in polymer molecular weight with time, nearly monodisperse polymer samples, and overall kinetics determined by propagation alone. These features are essential to permit precise control of the polymer structure.[26] In these controlled polymerizations the decrease in monomer concentration displays first-order decays and $k_{obs} = k_p[C]_0$, where k_p is the rate constant for propagation. Clearly, the polymerization mechanism of ionically functionalized RCOTs by **1** is much different, likely deriving from a multifaceted balance of initiation, propagation, and termination steps, each potentially influenced by anion coordination or ion pairing/clustering equilibria and polymer precipitation.

The central observations characterizing the polymerization of ionically functionalized RCOTs by **1** are (i) slow initiation relative to propagation, (ii) first-order monomer decays characterized by the empirical rate law eq 1, (iii) PDI ≈ 1.3−1.6 independent of the extent of the reaction or reaction conditions (studies on $\mathbf{M_A}$), (iv) $\bar{M}_n^{app}$ that is independent of the initial monomer and catalyst concentration and quickly plateaus becoming independent of the extent of the reaction (studies on $\mathbf{M_A}$), and (v) inhibition by the addition of a nonpolymerizing salt (studies on $\mathbf{M_C}$). Although a detailed mechanistic description is not yet possible, the basic features giving rise to these observations are qualitatively discussed below.

Slow initiation relative to propagation is implied by the absence of a H_α resonance, or other NMR signature, corresponding to the propagating species during polymerizations run to complete monomer conversion. The observation of slow initiation compared to propagation is similar to that observed for the ROMP of other RCOTs by **1** and analogous tungsten imido alkylidene catalysts. In these reports, polymerization is initiated by a small portion, usually 10−30%, of the originally added catalyst with no further description of the active propagating catalyst provided.[5,6] Slow initiation relative to propagation is not surprising. The catalyst **1** is somewhat unusual among tungsten and molybdenum imido alkylidene complexes. The majority of well-defined catalysts employed in ROMP are either 14 e^-, four-coordinate or 16 e^-, five-coordinate complexes in which the syn rotamer is the more thermodynamically stable form.[1] The catalyst used in this study is an 18 e^-, six-coordinate species (labile THF coordinated) with the anti rotamer stabilized by coordination of the *o*-methoxy group. Displacement of the *o*-methoxy ligand accompanies the first insertion. Therefore, a noteworthy difference between the uninitiated catalyst and the propagating species is the difference in coordinative and electronic saturation. This difference alone could account for the observed difference in reactivity of the uninitiated and propagating species. Additionally, the rates of reactivity of tungsten and molybdenum imido alkylidene complexes are often heavily influenced by the relative rates of reactivity of the syn and anti rotamers and the rate constants for their interconversion.[1,3,27−29] The anti rotamer is generally more reactive than the syn rotamer for tungsten and molybdenum alkylidene catalysts, but their relative reactivities are specific to the catalyst, monomer, and reaction conditions employed.[1,30] Here, the stabilization of the anti form of the uninitiated catalyst would slow the interconversion to the syn form. If the syn form were more reactive toward monomer insertion, the decrease in the relative concentration of the syn rotamer could account for the observed difference in relative reactivities.

The polymerization of ionically functionalized RCOTs is notable in that, at least for $\mathbf{M_A}$, the $\bar{X}_n$ is largely independent of the extent of the reaction and reaction stoichiometry. The constancy of $\bar{X}_n$ suggests either that the rates of propagation and termination are balanced or that a separate influence such as precipitation is limiting $\bar{X}_n$. Furthermore, the constancy of $\bar{X}_n$ also suggests that the unusual kinetics embodied in the empirical rate law eq 2 are due primarily to the details of initiation.

Precipitation provides a logical explanation for the independence of $\bar{X}_n$ on reaction stoichiometry. Slowed diffusion of reactants is expected to substantially decrease propagation for precipitated species, thereby acting as an effective termination step. Slowed propagation in a precipitated phase relative to solution kinetics has been observed, for instance, in the radical polymerizations of methyl methacrylate in cyclohexane, a nonsolvent for poly(methyl methacrylate).[31] With precipitation, the solution remains biphasic, and the much faster propagation for freshly initiated, soluble chains would be expected to dominate the overall reaction kinetics.

Precipitation also provides a logical explanation for the relatively narrow polydispersities and low molecular weights observed. The observed polydispersity (PDI ≈ 1.5) is more narrow than would be expected for a simple chain polymerization yielding a single polymer molecule per kinetic chain. For such a polymerzation, the polydispersity index rapidly increases with $\bar{X}_n$ toward a limiting value of 2.0, with a value of 1.9 already achieved at $\bar{X}_n = 10$. By effectively terminating the polymerization at a critical chain length for solubility, precipitation could offer a narrowing mechanism. Precipitation also provides a potential explanation for the much lower molecular weights observed relative to similar nonionically functionalized poly(RCOT)s. Even allowing for substantial error due to the use of relative standards, the molecular weights observed for $\mathbf{P_A}$ are much lower than has been reported for the polymerization of similar nonionic RCOTs by **1**. For instance, the polymerization of [2-(*tert*-butyldimethylsiloxy)-*n*-propyl]COT has been reported to yield number-average

molecular weight values as high as 746 000 when compared to PS in toluene.[32]

The most characteristic feature of the overall reaction kinetics for the polymerization of ionically functionalized RCOTs with **1** is the observed first-order decay in monomer concentration with k_{obs} proportional to the inverse of the *initial* monomer concentration (eq 1) and the inhibition by the addition of TBAOTf. Precedence for such behavior comes from two primary sources: (i) studies on the addition of Lewis bases to transition metal alkylidene catalysts such as **1**[2,15,32] and (ii) ion-pairing effects in ionic polymerizations.[17] In terms of the ROMP of ionically functionalized monomers by **1**, this precedence suggests two possible mechanisms for inhibition: (i) coordination of the weakly basic anion to the metal center or (ii) ion pairing/clustering influencing the activity of the monomer. In terms of kinetics, the two can basically act in the same manner by limiting the availability of reactive species. Equilibria involving anion coordination to the metal center or ion clustering could be imagined to inhibit the reaction if either the coordinated metal center or a tight ion pair, respectively, were less reactive than their free counterparts. Below each of these two mechanisms is discussed. The discussion focuses on the initiation step as it is currently hypothesized to dominate the kinetics of the system. The basic effects, however, could be easily incorporated into a more complex kinetic scheme treating initiation, propagation, and termination collectively. To recover the empirical rate law eq 2, a key assumption has to be made in dealing with both scenarios: the concentration of a critical ion is assumed to remain constant throughout the polymerization. Although the ionic centers are not destroyed during the polymerization, the activity of the ionic centers bound to polymer chains, especially in light of precipitation, is expected to differ from those of unpolymerized monomers. This oversimplification emphasizes the qualitative nature of the following discussion, as does the use of concentration where in certain cases activities would be more appropriate.

Alkylidene metathesis catalysts, such as **1**, are highly reactive toward a wide variety of functional groups and are known to coordinate a range of Lewis bases.[1,2,4,15] Metathesis polymerizations initiated by tungsten and molybdenum imido alkylidene catalysts in the presence of Lewis bases[2,15] have been shown to yield empirical rate laws similar to eq 2, raising the possibility that a similar mechanism may be at work here. For instance, Schrock and co-workers studied the polymerization of (*o*-(trimethylsilyl)phenyl)acetylene by molybdenum imido alkylidene complexes in the presence of Lewis bases such as lutidine and quinuclidine.[2] The kinetics of this system, in certain limits, was observed to follow eq 2 with $[S]_0$ replaced by the concentration of coordinating ligand present.

Equation 2 can be recovered by considering a reversible equilibrium between an active free catalyst and an inactive anion−coordinated catalyst as represented by the following sequence:

$$A^- + C \underset{k_{-1}}{\overset{k_1}{\rightleftharpoons}} AC^- \tag{3}$$

$$C + M \xrightarrow{k_i} CM \tag{4}$$

$$CM + (N-1)M \xrightarrow{\text{fast}} P \tag{5}$$

where C is the uncoordinated catalyst, A^- is the anion, and P is a polymer strand of length N. Equations 4 and 5 follow from the idea that initiation is rate limiting and that each initiation event yields a polymer strand of roughly constant chain length resulting in $\bar{X}_n = N$. Productive initiation competes with the nonproductive association. The extent of competition relates to the binding constant, $K = k_1/k_{-1}$, of the ligand to the catalyst. If reaction 4 is irreversible and $k_1, k_{-1} > k_i$, the following rate law is derived:

$$\frac{-d[M]}{dt} = \frac{k_i N [C]_{tot}[M]}{1 + K[A^-]} \tag{6}$$

where C_{tot} is the total unconsumed catalyst concentration ($[C]_{tot} = [C] + [AC^-]$). Equation 6 reduces to the empirical rate law eq 2, with $k = k_i N/K$, when the total unconsumed catalyst concentration is equal to the initial catalyst concentration ($[C]_{tot} = [C]_0$) as in the case of slow initiation, when $K[A^-] > 1$, and when anion concentration is independent of the extent of reaction and is given by the total available anion concentration ($[A^-] = [M]_0 +$ [added univalent salt]$_0$), thus neglecting ionic interactions and polymer precipitation.

Ion pairing and clustering in low dielectric constant media is known to influence a variety of chemical reactions.[16] In particular, ion pairing is essential in describing the kinetics of ionic polymerizations.[17] For instance, the addition of the dissociating sodium tetraphenylborate ($NaBPh_4$) to the anionic polymerization of styrene inhibits the polymerization by influencing the ion-pairing equilibrium involving the active chain end.[33] The reaction rate is observed to be inversely proportional to the concentration of the $NaBPh_4$ in a manner analogous to eq 6.

The empirically observed rate law (eq 2) can also be recovered by considering a reversible equilibrium involving the monomer between an active free ion and inactive ion pair:

$$M^{+/-} + Z^{-/+} \underset{k_{-1}}{\overset{k_1}{\rightleftharpoons}} MZ \tag{7}$$

$$C + M^{+/-} \xrightarrow{k_i} CM^{+/-} \tag{8}$$

$$CM^{+/-} + (N-1)M \xrightarrow{\text{fast}} P \tag{9}$$

where $M^{+/-}$ is the cyclooctatetraene ion of the monomer and $Z^{-/+}$ is the counterion. This is analogous to the treatment above except with the monomer involved in a preequilibrium instead of the catalyst. Under the assumptions analogous to those above, the rate equation (6) is recovered with $[A^-]$ replaced by $[Z^{-/+}] = [M]_0 +$ [added univalent salt]$_0$, $[C]_{tot}$ replaced by [C], and [M] replaced by $[M]_{tot}$, where $[M]_{tot}$ is the total unconsumed monomer concentration.

If we consider $\mathbf{M_C}$, for instance, the distinction between ion-pairing and anion coordination is a question of which interaction is stronger, triflate with its counterion (ion−ion interaction) or triflate with the metal center (ion−neutral). The ion-pairing mechanism appears more easily understood given the expectation for strong ion pairing in a low dielectric constant solvent such as $CHCl_3$.[34,35] Furthermore, the ^1H and ^{13}C NMR spectroscopic studies on **1** and its THF-free analogue do not provide evidence for a direct triflate−catalyst interaction. Although H_α for **1** is relatively insensitive to ligand coordination, C_α is much more sensitive. For

instance, there is a 8.7 ppm chemical shift difference for C_α between **1** and its THF-free analogue in $CDCl_3$, whereas there is a less than 0.1 ppm shift of H_α in $CDCl_3$. Addition of a 25-fold excess of TBAOTf to **1** resulted in a less than 0.5 ppm shift in C_α and no observable shift in H_α. Also supporting the ion-pairing mechanism over specific anion coordination is the observation that both the observed rate constant and the apparent order of monomer consumption during polymerization of the neutral monomer TMSCOT are unaffected by the addition of TBAOTf.

The above discussion is intended to provide a qualitative rationale for the observed rate law. The precise mechanism remains an open question with the notion of a bimolecular initiation step influenced by ion pairing of the monomer a first hypothesis. Ion−ion and ion−solvent interactions can substantially complicate the interpretation of kinetic data. The apparent first-order dependence on monomer and catalyst concentration could simply arise from changes in the ion activities rather than from a true bimolecular elementary step.[36] Regardless, the observed kinetics point out the distinctive features that can arise in the ROMP of ionically functionalized monomers using transition metal imido alkylidene catalysts. A more detailed understanding will require the study of an ionic monomer/catalyst system where the propagating species can be observed, the polymers formed are more amenable to molecular weight characterization, and the polymerizations are not complicated by precipitation. Such an understanding will be important in evaluating the potential of imido alkylidene complexes for the preparation of polyelectrolytes and the metathesis of other ionic monomers.

Experimental Section

Materials. All polymerization reactions are air- and moisture-sensitive and were performed in a nitrogen-filled drybox. Both monomers were thoroughly dried under vacuum (60 °C, 20 mTorr) for greater than 120 h. NMR spectra were recorded with a Varian INOVA 300 MHz spectrometer except where noted when a Varian INOVA 500 MHz spectrometer was used. Ultraviolet−visible absorption spectroscopy was performed on a Hewlett-Packard 8452A diode array spectrometer. Gel permeation chromatography was performed on a Waters chromatography system utilizing an HR4 size exclusion column, a 510 pump, and a 996 photodiode array detector with 0.4% (w/v) tetramethylammonium tetrafluoroborate ($TMABF_4$) in dimethyl sulfoxide (DMSO) as eluent. TMAPSS [PSS = poly(styrenesulfonate)] standards were prepared by ion exchange from narrow NaPSS standards (American Polymer Standards).

The tungsten catalyst, W=CH(*o*-C_6H_4OMe)(NC_6H_5)[$OCCH_3(CF_3)_2$]$_2$(THF) was prepared as described in the literature.[4] The preparation of the monomers, RCOT (R = TMS,[37] $CH_2CH_2SO_3TMA$,[13] and $CH_2CH_2NMe_3OTf$;[13] OTf = $CF_3SO_3^-$, TMA = Me_4N^+), is described in the literature. Toluene (Fisher) was distilled from sodium benzophenone. Chloroform (Fisher) and deuteriochloroform were distilled from calcium hydride and degassed by the freeze−pump−thaw method. For the GPC characterization of the polymers, DMSO and $TMABF_4$ were used as received.

Gravimetric Analysis of Polymerizations. The polymerizations were conducted according to the literature method.[13] A typical gravimetric analysis polymerization described for poly($COTCH_2CH_2NMe_3OTf$) follows.

$COTCH_2CH_2NMe_3OTf$ (706 mg, 2.1×10^{-3} mol) was added to a tared vial, followed by 6.8 g of $CHCl_3$ and **1** (27 mg, 3.3×10^{-5} mol). Upon addition of the catalyst, the vial was tightly capped and shaken vigorously. The reaction mixture was weighed into four tared vials, leaving a portion in the original vial. The reaction mixture in each vial was quenched with benzaldehyde at regular time intervals (0.5, 1, 2, 3, and 4 h). The resulting polymer was washed with $CHCl_3$ to remove unreacted monomer and benzaldehyde. The washes were filtered through a 0.2 μm syringe filter to recover polymer precipitate. The filters were first rinsed with $CHCl_3$ followed by DMSO to wash and then recover polymer from the syringe filter. The DMSO wash was returned to the appropriate reaction vial and concentrated. The polymer was dried at least 12 h under vacuum and weighed.

Polymerization Monitored by NMR Spectroscopy. Polymerizations to be monitored by NMR were conducted in Teflon-capped NMR tubes to exclude oxygen and moisture. The reagents were combined in a vial as described in the time−course polymerizations. A portion of the reaction mixture was then added to the NMR tube. The specifics of the polymerization of $COTCH_2CH_2SO_3TMA$ described in Figure 1 are detailed next.

$COTCH_2CH_2SO_3TMA$ (38.8 mg, 1.36×10^{-4} mol) and hexamethylbenzene (8.1 mg, 5.0×10^{-5} mol) were added to a tared vial followed by 1.64 g of $CDCl_3$. The vial was shaken to dissolve the monomer and standard, and then **1** (22.7 mg, 2.75×10^{-5} mol) was added. A portion of the reaction mixture was transferred by pipet to the NMR tube. The NMR instrument was programmed to acquire spectra at 10 min intervals.

Acknowledgment. This work was supported through the National Science Foundation CAREER Program (DMR-9703311), the Dreyfus New Faculty Program, the Beckman Young Investigator Program, and the University of Oregon. Partial support of the Center for Advanced Materials Characterization Laboratory (CAMCOR) at the University of Oregon was provided by the National Science Foundation (DMR-9601813) and the M. J. Murdock Charitable Trust.

References and Notes

(1) Schrock, R. R. *Tetrahedron* **1999**, *55*, 8141−8153.
(2) Schrock, R. R.; Luo, S.; Lee, J.; Jesse, C.; Zanetti, N. C.; Davis, W. M. *J. Am. Chem. Soc.* **1996**, *118*, 3883−3895.
(3) Schrock, R. R.; DePue, R. T.; Feldman, J.; Schaverien, C. J.; Dewan, J. C.; Lui, A. H. *J. Am. Chem. Soc.* **1988**, *110*, 1423−1435.
(4) Johnson, L. K.; Frey, M.; Ulibarri, T. A.; Virgil, S. C.; Grubbs, R. H.; Ziller, J. W. *J. Am. Chem. Soc.* **1993**, *115*, 8167−8176.
(5) Gorman, C. B.; Ginsburg, E. J.; Grubbs, R. H. *J. Am. Chem. Soc.* **1993**, *115*, 1397−1409.
(6) Klavetter, F. L.; Grubbs, R. H. *J. Am. Chem. Soc.* **1988**, *110*, 7807−7813.
(7) Bazan, G. C.; Oskam, J. H.; Cho, H.-N.; Park, L. Y.; Schrock, R. R. *J. Am. Chem. Soc.* **1991**, *113*, 6899−6907.
(8) Schaverien, C. J.; Dewan, J. C.; Schrock, R. R. *J. Am. Chem. Soc.* **1986**, *108*, 2771−2773.
(9) O'Dell, R.; McConville, D. H.; Hofmeister, G. E.; Schrock, R. R. *J. Am. Chem. Soc.* **1994**, *116*, 3414−3423.
(10) Schitter, R. M. E.; Jocham, D.; Stelzer, F.; Moszner, N.; Volkel, T. *J. Appl. Polym. Sci.* **2000**, *78*, 47−60.
(11) Zhang, N.; Wu, R.; Li, Q.; Pakbaz, K.; Yoon, C. O. *Chem. Mater.* **1993**, *5*, 1598−1599.
(12) Wagaman, M. W.; Grubbs, R. H. *Macromolecules* **1997**, *30*, 3975−3985.
(13) Langsdorf, B. L.; Zhou, X.; Adler, D. H.; Lonergan, M. C. *Macromolecules* **1999**, *32*, 2796−2798.
(14) Zhou, X.; Langsdorf, B. L.; Jones, F. E.; Lonergan, M. C. *Inorg. Chim. Acta* **1999**, *294*, 207−213.
(15) Wu, Z.; Wheeler, D. R.; Grubbs, R. H. *J. Am. Chem. Soc.* **1992**, *114*, 146−151.
(16) *Ions and Ion Pairs in Organic Reactions;* Szwarc, M., Ed.; Wiley: New York, 1974; Vol. 2.
(17) Szwarc, M. In *Ions and Ion Pairs in Ionic Polymerization*; Szwarc, M., Ed.; Wiley: New York, 1974; Vol. 2, pp 375−446.
(18) Kraft, R.; Muller, A. H. E.; Warzelan, V.; Hocker, H.; Schulz, G. V. *Macromolecules* **1978**, *11*, 1093.
(19) Ise, N.; Matsui, F. *J. Am. Chem. Soc.* **1968**, *90*, 4242−4247.
(20) Johnson, L. K.; Grubbs, R. H.; Ziller, J. W. *J. Am. Chem. Soc.* **1993**, *115*, 8130−8145.
(21) Schrock, R. R.; Feldman, J.; Cannizzo, L. F.; Grubbs, R. H. *Macromolecules* **1987**, *20*, 1169−1172.

(22) As with the polymerization of the ionic monomers, initiation is slow relative to propagation in the polymerization of TMS-COT with no discernible change observed in the alkylidene ^{1}H NMR resonance during the course of the polymerization.
(23) ^{1}H NMR experiments confirm linearity of first-order representation through greater than 90% conversion.
(24) Neither adjusting the ionic strength with TBAOTf in DMSO nor the addition of trifluoroacetic acid in DMSO individually or in combination provided a successful eluent.
(25) The initial aliquot corresponds to 18−28% conversion with a time interval of 7.5−30 min depending on the specific polymerization.
(26) Predictive control over polymer stereochemistry is achieved more through proper choice of catalyst features. See ref 1.
(27) Schrock, R. R.; Crowe, W. E.; Bazan, G. C.; DiMare, M.; O'Regan, M. B.; Schofield, M. H. *Organometallics* **1991**, *10*, 1832−1843.
(28) Oskam, J. H.; Schrock, R. R. *J. Am. Chem. Soc.* **1992**, *114*, 7588−7590.
(29) Oskam, J. H.; Schrock, R. R. *J. Am. Chem. Soc.* **1993**, *115*, 11831−1145.
(30) Schrock, R. R. *Acc. Chem. Res.* **1990**, *23*, 158−165.
(31) Hayden, P.; Melville, H. *J. Polym. Sci.* **1960**, *43*, 215−227.
(32) Moore, J. S.; Gorman, C. B.; Grubbs, R. H. *J. Am. Chem. Soc.* **1991**, *113*, 1704−1712.
(33) Schmitt, B. J.; Schulz, G. V. *Eur. Polym. J.* **1975**, *11*, 119−130.
(34) Islam, M. N.; Leffek, K. T. *J. Chem. Soc., Perkin Trans. 2* **1977**, *7*, 952−7.
(35) Kabisch, G. *Ber. Bunsen-Ges. Phys. Chem.* **1976**, *80*, 602−7.
(36) Hammett, L. P. *Physical Organic Chemistry: Reaction Rates, Equilibria, and Mechanism*, 2nd ed.; McGraw-Hill: New York, 1970.
(37) Cooke, M.; Russ, C. R.; Stone, F. G. *J. Chem. Soc., Dalton Trans.* **1975**, 256−259.

MA0020685